Article

On the Stability of Rubble Mound Structures under Oblique Wave Attack

Meysam Bali [1] **, Amir Etemad-Shahidi** [2,3,*] **and Marcel R. A. van Gent** [4,5]

1 Pouya Tarh Pars Consulting Company, Tehran 1437615613, Iran; meysam_baali@yahoo.com
2 Griffith School of Engineering and Built Environment, Griffith University, Mount Gravatt, QLD 4222, Australia
3 School of Engineering, Edith Cowan University, Joondalup, WA 6027, Australia
4 Department of Coastal Structures & Waves, Deltares, 2600 MH Delft, The Netherlands; marcel.vangent@deltares.nl
5 Department of Hydraulic Engineering, Delft University of Technology (TU Delft), 2628 CN Delft, The Netherlands
* Correspondence: a.etemadshahidi@griffith.edu.au

Abstract: Slope stability formulae for rubble mound structures are usually developed for head-on conditions. Often, the effects of oblique waves are neglected, mainly because it is assumed that for oblique wave attack, the reduction in damage compared to perpendicular wave attack is insignificant. When the incident waves are oblique, the required armour size can be reduced compared to the perpendicular wave attack case. Therefore, it is important to consider the wave obliquity influence on slope stability formulae as a reduction factor. One of the most recent formulae for estimating the stability of rock-armoured slopes, referred to as Etemad-Shahidi et al. (2020), was proposed for perpendicular wave attack. The aim of this study is to develop a suitable wave obliquity reduction factor for the above-mentioned stability formula. To achieve this, first, laboratory experiment datasets from existing reliable studies were selected and analysed. Then, previously suggested reduction factors were evaluated and a suitable reduction factor for the mentioned stability formula were suggested. The suggested reduction factor includes the effect of wave obliquity and directional spreading explicitly. It is shown that the stability prediction is improved by using the wave obliquity reduction factor.

Keywords: oblique wave; rubble mound breakwater; slope stability; reduction factor

1. Introduction

Many studies are being conducted on breakwaters and especially new breakwaters [1–7]. However, studies in the field of rubble mound breakwaters have not stopped yet, and many studies are still being conducted in different fields of rubble mound breakwaters [8–11]. One of the most important issues in breakwater design is the determination of the armour block's weight using the stability number N_s. Stability formulae for armour layers of rubble mound structures are typically based on laboratory experiments in wave flumes, i.e., 2D experiments. Therefore, the formulae are generally developed for perpendicular wave attack and do not include effects of oblique waves. This is, however, a conservative assumption since the stability of armour slopes generally increases for oblique waves. Waves usually attack breakwater obliquely, and it is important to find out how much the stability increases due to the wave obliquity. Oblique wave attack does not only affect the stability of armour layers, but also wave overtopping. To account for the effects of oblique waves on mean overtopping discharges, several studies have been conducted [12–16]. In most of them, a reduction factor for wave obliquity has been proposed to mean overtopping discharges.

Several studies have been performed to investigate the effect of wave angle (β) on armour stability. A few researchers have performed laboratory experiments to consider

effects of oblique waves on the stability of armour layers. They performed tests with long-crested and/or short-crested waves on rock and/or concrete armour layers. Almost all test results showed that for oblique waves, smaller units are required. Therefore, they proposed a reduction factor (γ_β) in the required armour size. This reduction factor has been found to be a function of ($\cos^X \beta$). Galland [13] carried out tests with long-crested waves and incident waves with angles between $\beta = 0°$ and $75°$ and proposed $X = 0.25$. Yu et al. [17] performed tests with long-crested and short-crested waves with angles between $\beta = 0°$ and $60°$ on rock and suggested $X = 1.16$. Wolters and Van Gent [18] also provided a dataset for wave angles up to $\beta = 70°$ for rock and they obtained $X = 1.1$, which is very close to that suggested by Yu et al. [17]. In the last study, Van Gent [19] performed small-scale tests in a wave basin to assess the effects of oblique waves on the stability of rock slopes and armoured cubes. The physical model experiments were focused on wave directions between perpendicular ($0°$) and parallel ($90°$) using both short- and long-crested waves. They showed that that for rock slopes, the influence of oblique waves is larger for long-crested waves. Table 1 shows the wave obliquity reduction factor for rock armour stability from various authors. This table shows that Galland [13] indicates a much smaller influence of wave obliquity compared to other studies. Moreover, in the approach by Van Gent [19], a minimum value for the reduction factor was suggested for parallel waves with wave angle of $90°$. In fact, when waves are parallel to the longitudinal axis of the structure, the reduction factor is limited to 0.42 and 0.35 for short-crested and long-crested waves, respectively.

Table 1. Wave obliquity reduction factor for rock armour size from various studies.

Reference	Formula		Equation No
Galland [13]	$\cos^{0.25} \beta$		(1)
Yu et al. [17]	$\cos^{1.157} \beta$		(2)
Wolters and Van Gent [18]	$\cos^{1.1} \beta$		(3)
Van Gent [19]	$(1 - c_\beta) \cos^2 \beta + c_\beta$	$c_\beta = 0.42$ for short-crested $c_\beta = 0.35$ for long-crested	(4)

Figure 1 shows the graphical presentation of wave obliquity reduction factor suggested in different references. As discussed before, Galland [13] indicates the lower influence of wave obliquity. In the range of $0 < \beta < 45$, the prediction of wave obliquity reduction factor by Yu et al. [17], Wolters and Van Gent [18] (WV) and Van Gent [19] (VG) are very similar, and for angles more than $50°$ degrees, they become different. For $\beta > 45$, Yu et al. [17] and WV predict a much higher influence of the wave obliquity on armour size than that of Van Gent [19] for rock slopes.
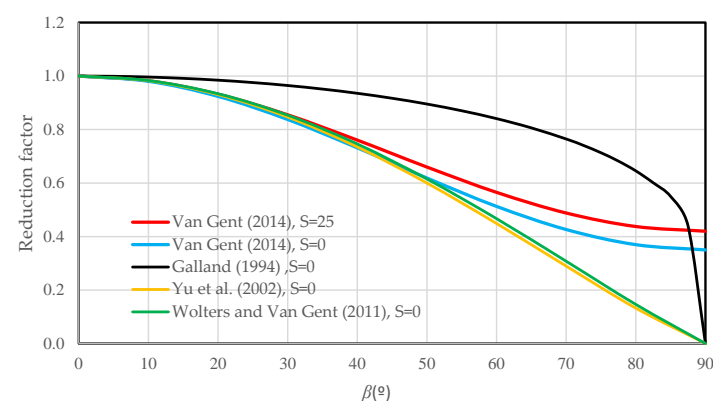

Figure 1. Comparison of methods describing the influence of oblique waves on armour size. Red and blue line: Van Gent [19], black line: Galland [13], yellow line: Yu et al. [17] and green line: Wolters and Van Gent [19].

There are several experimental formulae for the predication of stability number [1,20–23]. They have been generally developed for perpendicular wave attack without considering the wave obliquity effects. The suggested reduction factors (γ_β) are compatible with a specific stability formula. For example, the formula proposed by Yu et al. [17] is compatible with Hudson's [20] stability formula, i.e.:

$$N_s = \frac{H_s}{\Delta D_{n50}} = (K_D cot\alpha)^{1/3} \tag{5}$$

where N_s is the stability number, D_{n50} is the nominal diameter of the stones, H_s is the significant wave height, α is the structure front angle, $\Delta = \rho_a/\rho_w - 1$ is the relative buoyant density, ρ_a is the armour density and ρ_w is the density of water. The stability coefficient, K_D, incorporates the effects of armour type and safety factor, and it varies from 2 (1.6) for breaking waves to 4 (2.8) for non-breaking waves hitting the trunk (head) of a breakwater. Van Gent's [19] reduction factor is compatible with Van Gent et al.'s [22] rock armour stability formula, i.e.,:

$$N_s = 8.4 P^{0.18} Ir_{m-1,0}^{-0.5} \left(S_d / \sqrt{N_w}\right)^{1/5} (H_s / H_{2\%}) \quad \text{If} Ir_{m-1,0} < Ir_c \text{ or } cot\alpha \geq 4 \tag{6a}$$

$$N_s = 1.3 P^{-0.13} Ir_{m-1,0}^{P} cot\alpha^{0.5} \left(S_d / \sqrt{N_w}\right)^{1/5} (H_s / H_{2\%}) \quad \text{If} Ir_{m-1,0} \geq Ir_c \text{ and } cot\alpha < 4 \tag{6b}$$

with $Ir_c = (6.46 P^{0.31} tan\alpha^{0.5})^{1/(P+0.5)}$.

In this equation, P is the permeability, $H_{2\%}$ is the average of the highest 2% of incident waves, S_d is the damage level, N_w is the number of waves and $Ir_{m-1,0}$ is the Iribarren number using $T_{m-1,0}$ (the spectral mean energy period). Equation (6a,b) were applied for the plunging and surging condition, respectively.

One of the most recent formulae for the calculation of rock stability number is Etemad-Shahidi et al.'s [1], hereafter EBV, shown below:

$$N_s = 3.9 C_p N_w^{-1/10} S_d^{1/6} Ir_{m-1,0}^{-1/3} \quad \text{If } Ir_{m-1,0} \geq 1.8 \quad \text{(surging waves)} \tag{7a}$$

$$N_s = 4.5 C_p N_w^{-1/10} S_d^{1/6} Ir_{m-1,0}^{-7/12} \quad \text{If } Ir_{m-1,0} < 1.8 \quad \text{(plunging waves)} \tag{7b}$$

where C_p is the coefficient of permeability defined as $[1 + (D_{n50c}/D_{n50})^{3/10}]^{3/5}$ and D_{n50c} is the median nominal size of the core material. An extensive database from different sources was used to develop this formula. Moreover, this formula is based on the local significant wave height and spectral mean energy period of the incident waves. In addition, instead of permeability, it includes effects of the relative size of core material and is more accurate than other formulae [1].

The main aim of this paper is to investigate effect of the wave obliquity/spreading and extending EBV formula by considering the effect of wave angle and spreading coefficient. To achieve this, first, all existing new reduction factors (Galland [13], Yu et al. [17], Wolters and Van Gent [18] and Van Gent [19]) were examined (in combination with the EBV formula).

For this purpose, the Van Gent [19] dataset (170 records) was used for the development of the new reduction factor, and the Yu et al. [17] dataset (70 records) was used for its evaluation.

2. Methodology

All the used tests are cumulative, while stability formulae are generally based on rebuilt tests. Hence, they need to be adjusted to convert cumulative test results to rebuilt ones first. This adjustment can be achieved by adjusting the number of waves (e.g., Van der Meer and Sigurdarson, 2016). For each of the sea states, the S_d–N_w relationship can be calculated using Equation (7a,b). The estimation of N_{w1-2}, the number of added waves in test 2 (second test in a cumulative test series), which results in the same damage as that of test 1, is required to convert the N_w of a cumulative test to that of a rebuilt one. Basically,

N_{w1-2} should be added to N_{w2} before estimating the damage using stability formulae. For surging waves, Equation (7a) can be written as:

$$S_d = 0.26^6 \, N_s^6 \, C_p^{-6} \, N_w^{0.6} \, Ir_{m-1,0}^2 \text{ if } Ir_{m-1,0} \geq 1.8 \tag{8}$$

$$S_{d1} \sim N_{s1}^6 \, N_{w1}^{0.6} \, Ir_{1m-1,0}^2 \tag{9}$$

$$S_{d1} \sim N_{s2}^6 \, N_{w1-2}^{0.6} \, Ir_{2m-1,0}^2 \tag{10}$$

$$N_{s1}^6 \, N_{w1}^{0.6} \, Ir_{1\,m-1,0}^2 = N_{s2}^6 \, N_{w1-2}^{0.6} \, Ir_{2\,m-1,0}^2 \tag{11}$$

$$Nw_{1-2} = (N_{s1}/N_{s2})^{10} \, (Ir_{1\,m-1,0}/Ir_{2\,m-1,0})^{20/6} \times N_{w1} \tag{12}$$

$N_{s2}/N_{s1} = k$ (as $H_{s2} = k \, H_{s1}$), and assuming $Ir_{1m-1,0} \approx Ir_{2m-1,0}$ (constant wave steepness test series), then $Nw_{1-2}/Nw_1 = (1/k)^{10}$. k is commonly about 1.20, i.e., a 20% increase in the wave height in the test series. For $1.10 < k < 1.30$, the estimations of N_{w1-2}/N_{w1} and ΔS_d are listed in Table 2.

Table 2. The relation of N_{w1-2}/N_{w1} and ΔS_d by assuming $N_{w1} = N_{w2}$ and $Ir_{1m-1,0} \approx Ir_{2m-1,0}$.

k	1.10	1.15	1.20	1.25	1.30
Nw_{1-2}/Nw_1 (%)	39	25	16	11	7
ΔS_d (%)	21.6	14.3	9.3	6.5	4

The second row shows that N_{w1-2}/N_{w1} is about 16% (assuming $k = 1.2$). In other words, the (cumulative) damage in the second test is due to $N_{w2} + 0.16 \, N_{w1} = 1.16 \, N_{w2}$.

The last row shows the change in the S_d if the tests were non-cumulative/rebuilt (assuming that $N_{w1} = N_{w2}$ and noting that $S_d \sim N_w^{0.6}$). For example, if $k = 1.2$, then $\Delta S_d = (1 + 0.16)^{0.6} - 1 = 9.3\%$. In other words, the damage in the second test is 9.3% more than that in a rebuilt test (with the same number of waves), and N_s would differ about 20%.

The Van der Meer formula [21] can also be applied to such situations via the cumulative damage method, which has been described in Van der Meer [24] and later in the Rock Manual [25], and which has also been implemented in Breakwat. In fact, the method is quite straightforward. The first sea state, characterised by a significant wave height H_{s1}, mean period T_{m1} and number of waves N_{w1}, yields a calculated damage level S_{d1}. The second sea state would be defined by H_{S2}, T_{m2} and N_{w2}. The next step is to determine the number of waves (N_{w12}) required for the second sea state to induce the same level of damage (S_{d1}) caused by the first sea state. Subsequently, the damage for the second sea state (S_{d2}) can be calculated by applying ($N_{w1-2} + N_{w2}$) as the total number of waves.

More discussion about conversion of cumulative-to-rebuilt damage is described in van der Meer and Sigurdarson [26].

After this modification, tests with very low damage levels ($S_d < 2$) and very high damage levels ($S_d > 12$), which are less common in practice [25,27] (e.g., Rock Manual, 2007, CEM, 2011), were excluded. In this way, a total of 77 records were selected for further processing. A brief description of the range of governing parameters based on β (0°, 15°, 30°, 45°, 60°, 70°, 80° and 90°) and S (0, 10, 25 and 40) ranges is presented in Tables 3 and 4, respectively. Note that for the tests with directional spreading, the amount of directional spreading is described by S, where $S = 0$ corresponds to long-crested waves.

Table 3. Range of parameters used for formula development based on the β range.

Parameter	β							
	0	15	30	45	60	70	80	90
N_w	1000	1000	1000	1000	1000	1000	1000	1000
$cot\alpha$	1.5	1.5	1.5	1.5	1.5, 2	1.5, 2	1.5, 2	1.5
D	1.7	1.7	1.7	1.7	1.7	1.7	1.7	1.7
S	0–40	0–40	0–40	0–40	0–40	0–25	0–25	0–25
P	0.4, 0.5	0.4, 0.5	0.4, 0.5	0.1–0.5	0.1–0.5	0.1–0.5	0.1–0.5	0.1–0.5
$s_{om-1,0}$ ($\times 10^{-2}$)	3–6	3–6	3–6	3–6	3–6	3–6	3–6	3–6
$Ir_{m-1,0}$	2.7–3.6	2.6–3.6	2.6–3.5	2.6–3.6	2.2–3.7	2.3- 4.0	2.2–3.0	3.1–3.5
h/H_s	3.4–10.5	3.0–14.7	3–8.0	2.6–11.0	2.4–14.5	2.7–11.3	4.6–6.5	5.5–5.9
D_{n50c}/D_{n50}	0.4–0.43	0.4–0.43	0.4–0.43	0–0.43	0–0.43	0–0.43	0–0.43	0.0–0.43
S_d	2–7.1	2.2–11.5	2.3–6.5	2.0–7.0	2.0–8.8	2–12	2.2–9.2	3.4–3.7
N_s	1.7–3.0	1.2–3.4	2.3–3.42	2.0–3.4	1.7–4.7	2.2–4.8	3.8–5.4	4.2–4.5

Table 4. Range of parameters used for formula development based on the *S* range.

Parameter	S			
	0	10	25	40
N_w	1000	1000	1000	1000
$cot\alpha$	1.5, 2	1.5	1.5, 2	1.5
D	1.7	1.7	1.7	1.6
β	0–90	0–45	50–70	0–45
P	0.1–0.5	0.4	0.1–0.5	0.4
$s_{om-1,0}$ ($\times 10^{-2}$)	3–6	3–6	3–6	3–6
$Ir_{m-1,0}$	2.2–4.0	2.6–2.7	2.2–3.3	2.6–2.7
h/H_s	2.4–14.7	3.0–4.0	5.3–14.1	3–3.76
D_{n50c}/D_{n50}	0.0–0.43	0.40	0.0–0.43	0.40
S_d	2–11.5	2–6.5	2.3–6.5	2.1–7.2
N_s	1.2–5.4	2.5–3.4	2.5–3.4	2.7–3.4

3. Results and Discussion

First, the Galland [13], Yu et al. [17], Wolters and Van Gent [18] and Van Gent [19] reduction functions in combination with the EBV stability formula were evaluated. Then, an attempt was made to find an appropriate and compatible reduction factor for the EBV stability formula. Figures 2–5 show the comparison of observed and predicted stability numbers using existing reduction factors. As seen, the Van Gent [9] one is more appropriate compared to the other reduction factors. As discussed before and shown in Figure 1, for $\beta > 45$, Yu et al. [17] and WV predict a much higher influence of the wave obliquity on rock size (reduction in armour size) and stability number (increase in the stability number) compared to Van Gent [19].

Next, we attempted to derive a compatible reduction factor for applications in combination with the EBV stability formula.

Figure 6a shows that the $f(\beta) = N_{s\,EBV}/N_{s\,Measured}$ versus β. As seen $N_{s\,EBV}/N_{s\,Measured}$ is scattered. For example, $N_{s\,EBV}/N_{s\,Measured}$ is between 0.4 and 0.8 for $\beta = 60°$. Moreover, some records for relatively small wave angles and long-crested waves ($S = 0$) result in reduction factors larger than 1, and some data points at $\beta = 0°$ are not close to 1. The values larger than 1 for perpendicular waves are due to differences between the stability expression and the data. The data point with a gamma value larger than 1 for a wave angle of 15 degrees, larger than for perpendicular waves, is based on low damage values (Sd = 2.2 for perpendicular waves). For low damage values, there is a natural larger relative spreading in the results due to the dependency of the damage values on the (in)stability of only a few stones.
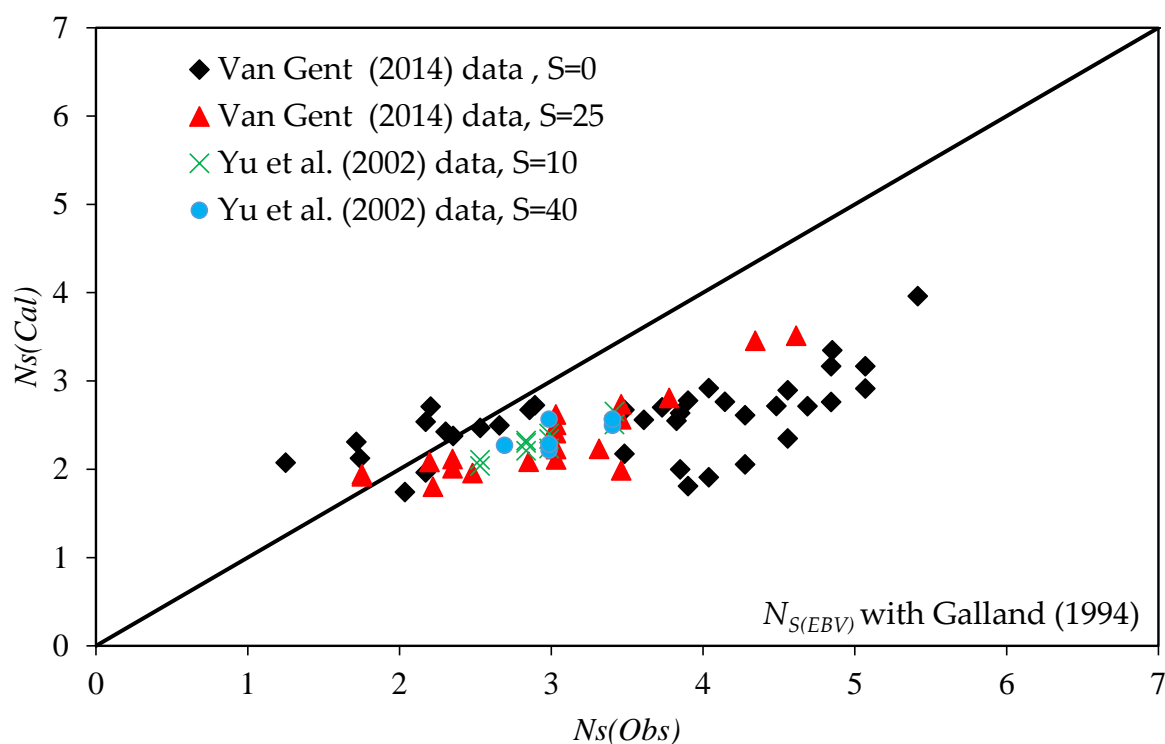
Figure 2. Comparison between measured and calculated stability number using EBV with Galland reduction factors. Black diamond and red triangle: Van Gent [19], green multiplication and blue circle: Yu et al. [17].
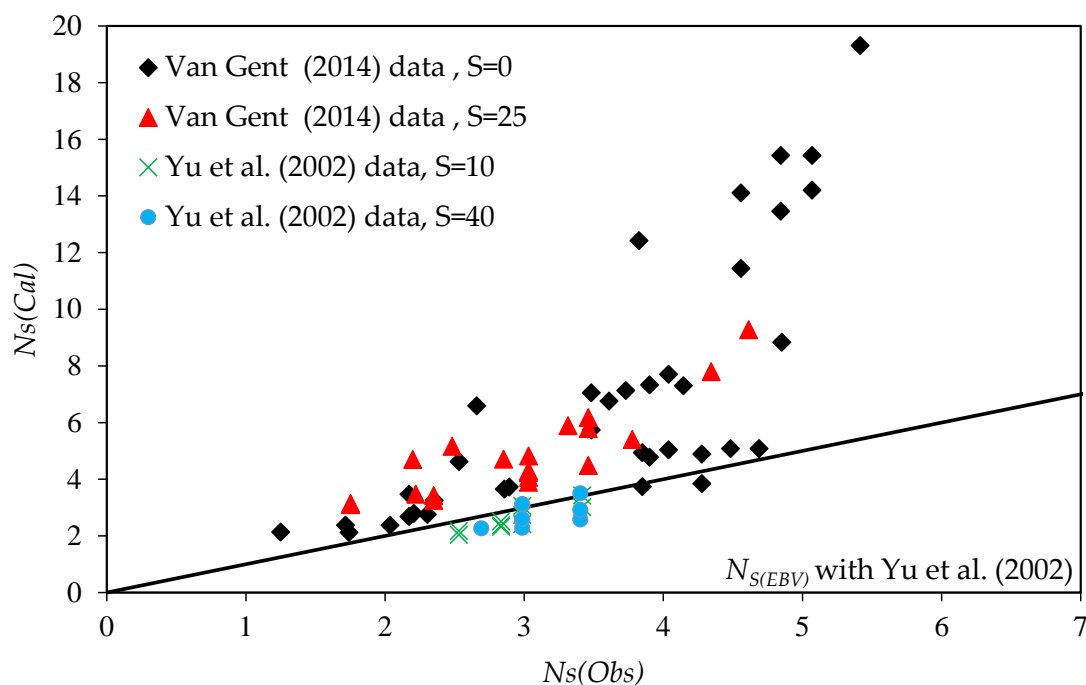

Figure 3. Comparison between measured and calculated stability number using EBV with Yu et al. [17] reduction factors. Black diamond and red triangle: Van Gent [19], green multiplication and Blue circle: Yu et al. [17].
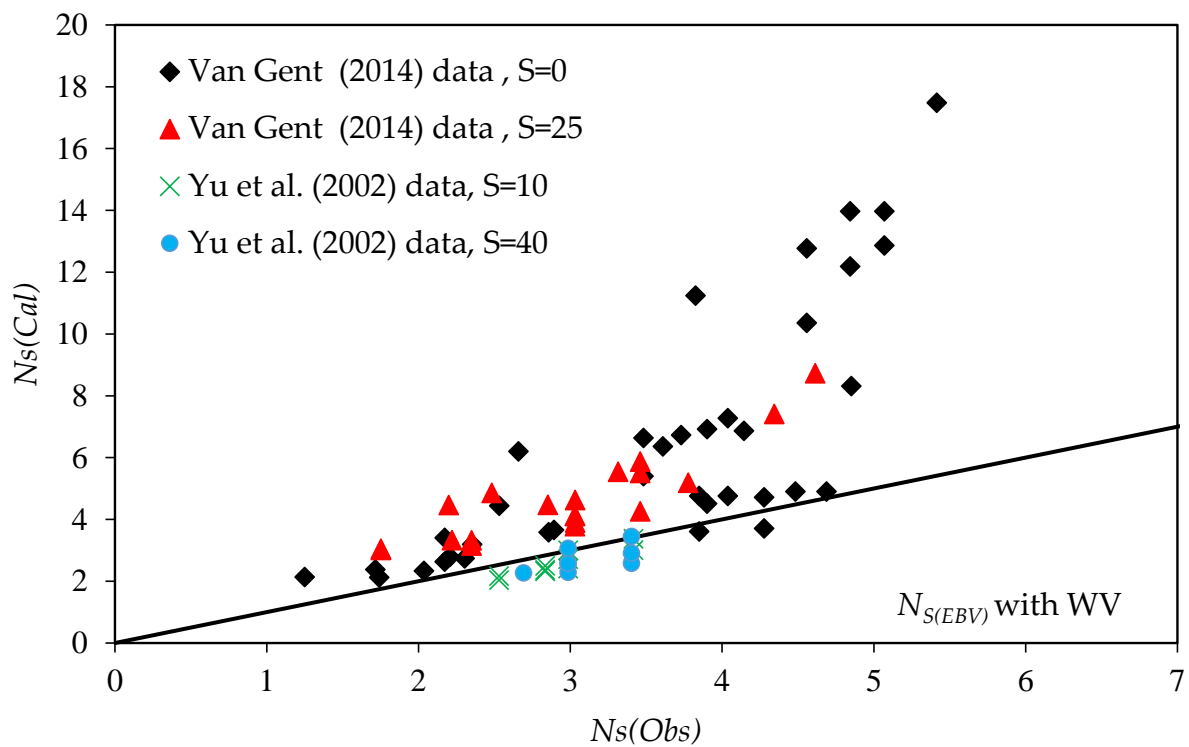
Figure 4. Comparison between measured and calculated stability number using EBV with Wolters and Van Gent [18] reduction factors. Black diamond and red triangle: Van Gent [19], green multiplication and blue circle: Yu et al. [17].
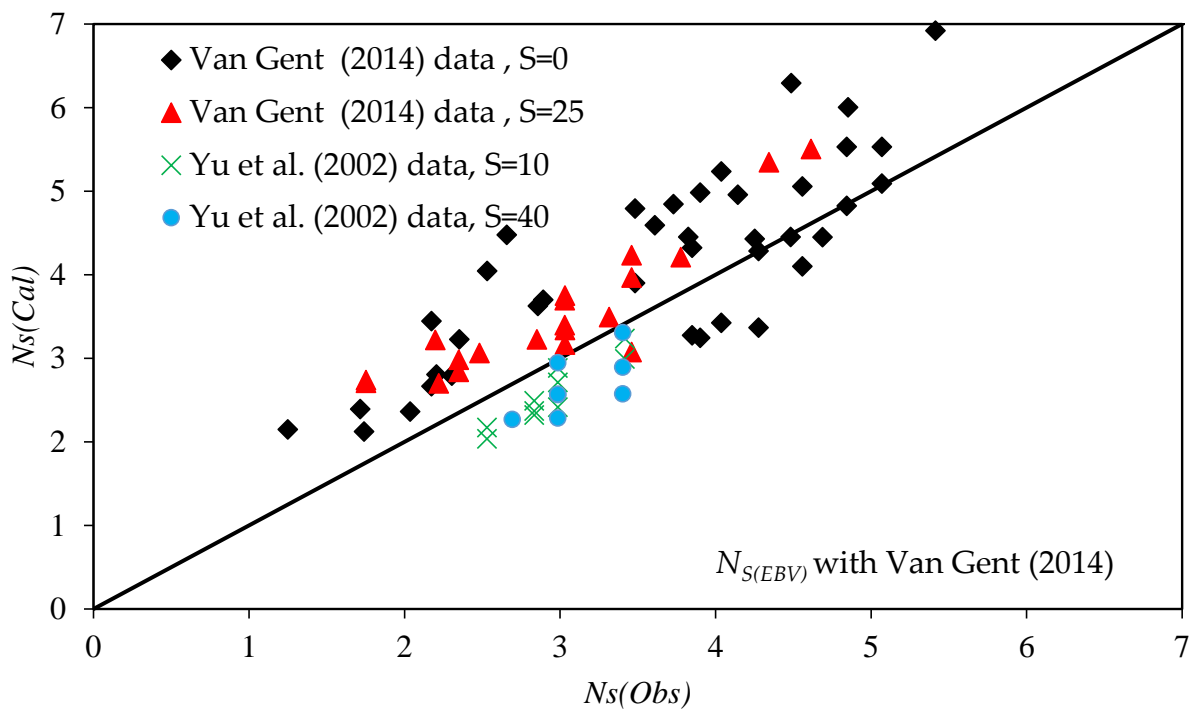

Figure 5. Comparison between measured and calculated stability number using EBV with Van Gent [19] reduction factors. Black diamond and red triangle: Van Gent [19], green multiplication and blue circle: Yu et al. [17].
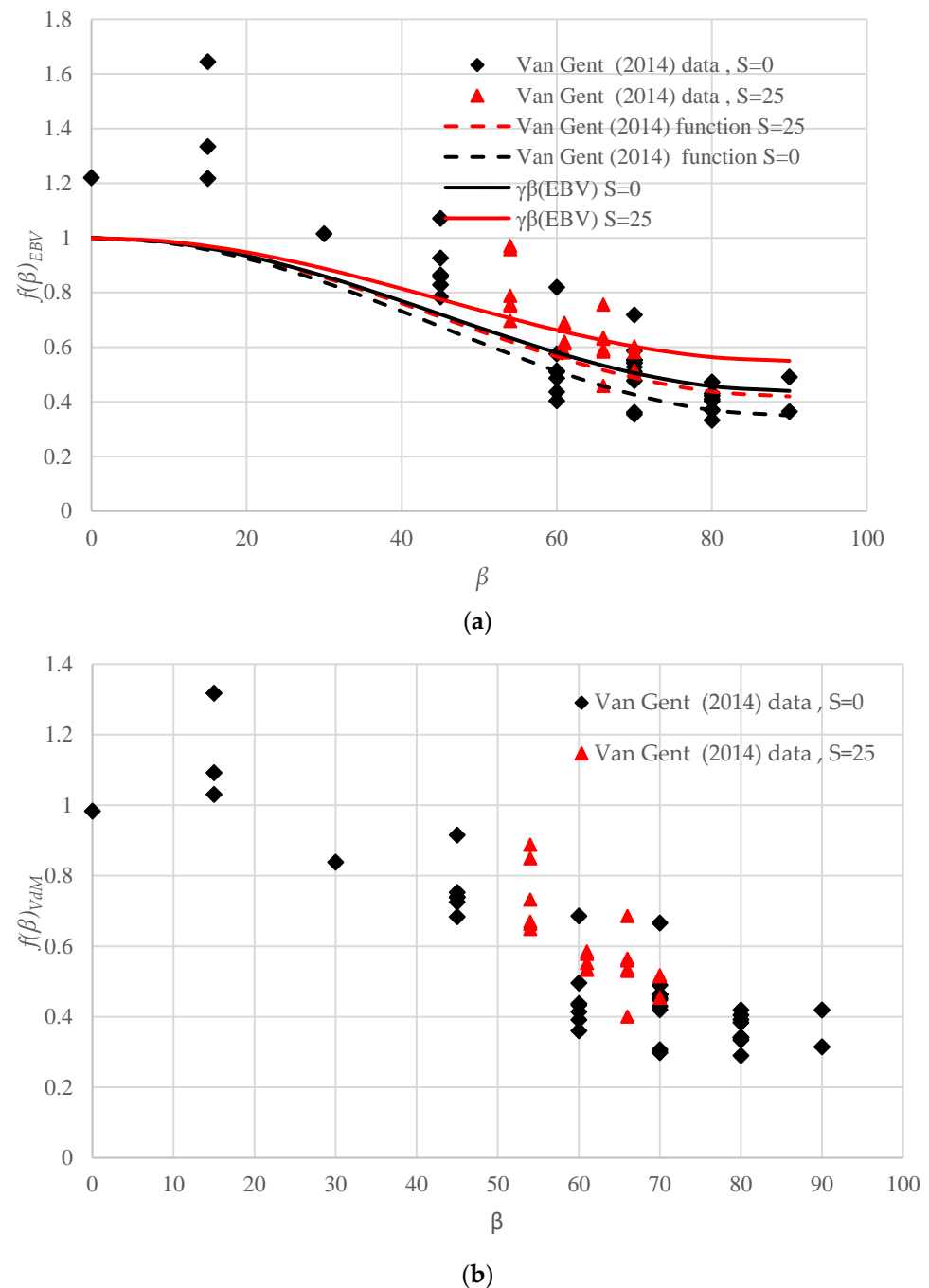
(**a**)

(**b**)

Figure 6. (**a**) Variation in $f(\beta)_{EBV}$ versus β, (**b**) variation in $f(\beta)_{VSK}$ versus β. Black diamond, red triangle: Van Gent [19].

It should be mentioned that this is not because of using $N_{S\ EBV}$ for stability; the issue exists when using other stability formulae. For example, in Figure 6b, the VSK formula was applied and data points at $\beta = 0°$ are not close to 1. It was found that to derive a more appropriate and compatible reduction factor for the EBV stability formula, the Van Gent [19] reduction function can be used with a modified c_β value. Using the Van Gent [19] approach, the optimal c_β values are 0.54 and 0.44 for short- and long-crested waves, respectively. Therefore, the reduction factor for the EBV stability formula can be proposed to be:

$$\gamma_{\beta\ EBV} = (1 - c_\beta)\cos^2\beta + c_\beta \quad c_\beta = 0.44\ (0.54) \text{ for long (short) crested waves} \tag{13}$$

Figure 6a shows the comparison of Van Gent [19] and the reduction factor calibrated for the EBV formula versus β. As seen, using a modified c_β for application in combination with the EBV stability expression indicates less influence of wave obliquity compared to that suggested by Van Gent [19] in combination with another stability formula.

Figure 7 shows the comparison between the measured and predicted stability numbers using the new wave obliquity reduction factor. As seen, the scatter in the data is reduced in this way. In addition, most of the data points are concentrated on the line of the perfect agreement when using EBV with a new reduction factor predicts the stability much better than others' formulae.
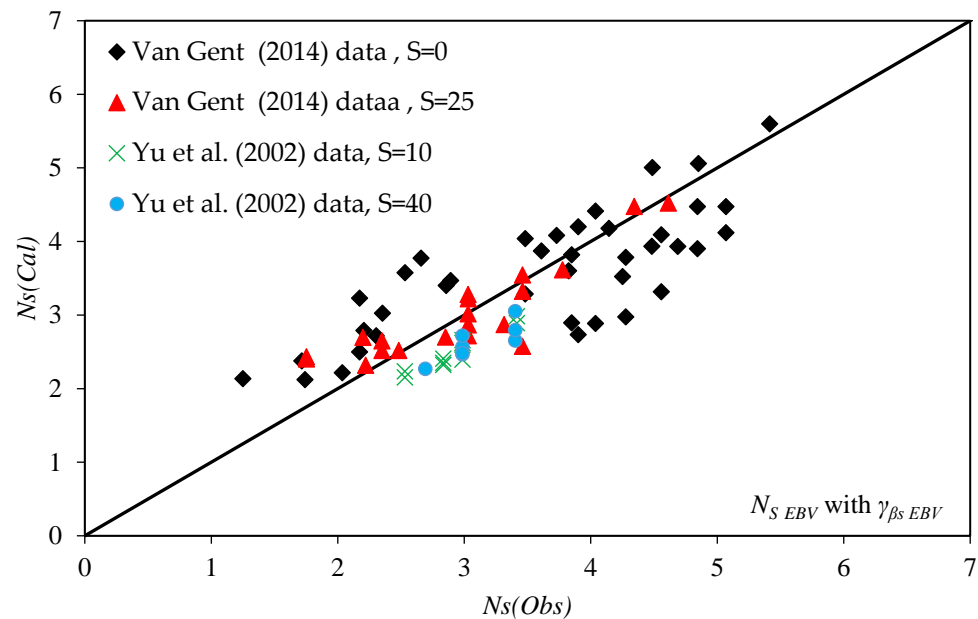

Figure 7. Comparison between measured and predicted (by EBV) stability numbers using the new reduction factor ($\gamma_{\beta \ EBV}$). Black diamond and red triangle: Van Gent [19], green multiplication and Blue circle: Yu et al. [17].

The performances of the various formulae were also evaluated quantitatively using accuracy metrics such as the normalised bias (*NBias*), the scatter index (*SI*) and the correlation coefficient (*CC*), defined below:

$$NBias = \frac{1}{n} \frac{\sum_1^n (p_i - m_i)}{\overline{m_i}} \times 100 \tag{14}$$

$$SI = \frac{\sqrt{\frac{1}{n}\sum_{i=1}^n (p_i - m_i)^2}}{\overline{m_i}} \times 100 \tag{15}$$

$$CC = \frac{\sum_{i=1}^n (p_i - \overline{p_i})(m_i - \overline{m_i})}{\sqrt{\sum_{i=1}^n (m_i - \overline{m_i})^2 (p_i - \overline{p_i})^2}} \tag{16}$$

where p_i and m_i denote the predicted and measured values, respectively. The number of measurements is n and the bar denotes the mean value.

Tables 5 and 6 display the accuracy metrics of the EBV stability formula using Van Gent [19] and the new reduction factor based on the Van Gent [19] and Yu et al. [17] datasets, respectively. As seen, the calibration of the coefficient in Equation (13) results in a negligible bias.

Table 5. Accuracy metrics of $N_{S\ EBV}$ using the new and Van Gent [19] wave obliquity reduction factors, Van Gent [17] data.

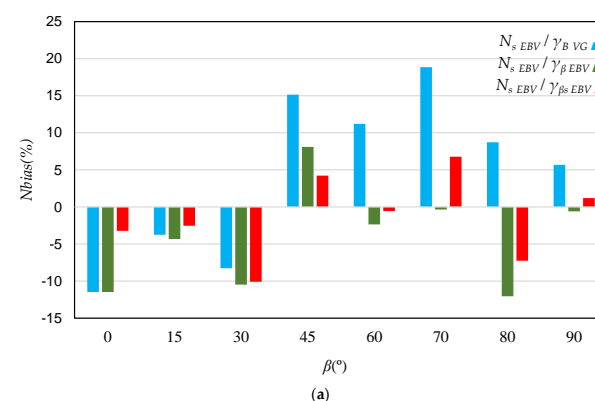|	$N_{s\ EBV}/\gamma_{B\ VG}$	$N_{s\ EBV}/\gamma_{\beta\ EBV}$	$N_{s\ EBV}/\gamma_{\beta s\ EBV}$
NBias	16.4	−0.05	−0.05
SI	24	17.7	17.70
CC	0.83	0.80	0.80

Table 6. Accuracy metrics of $N_{S\ EBV}$ using the new and Van Gent [19] wave obliquity reduction factors, Yu et al. [17] data.

	$N_{s\ EBV}/\gamma_{B\ VG}$	$N_{s\ EBV}/\gamma_{\beta\ EBV}$	$N_{s\ EBV}/\gamma_{\beta s\ EBV}$
NBias	−13	−16.0	−15.70
SI	15	16.85	16.10
CC	0.77	0.82	0.81

As seen, the new suggested reduction factor ($\gamma_{\beta\ EBV}$) considers the effect of wave angle (quantitatively) and wave spreading for short- and long-crested waves (qualitatively). Therefore, in the third step, a reduction coefficient ($\gamma_{\beta sEBV}$), which is a function of wave angle and spreading qualitatively, will be investigated.

As discussed in Yu et al. [17] and Van Gent [19], unidirectional (long-crested) and multidirectional (short-crested) oblique waves can affect the stability number differently. They concluded that more spreading leads to reducing the influence of wave obliquity. Here, the effects of wave directionality were reanalysed. Experiments by Yu et al. [17] included only tests with $S = 10$ and $S = 40$ as a measure for directional spreading. The usual minimum and maximum values of wave spreading are 0 and about 45, respectively. These extreme values are covered in the used datasets but with no intermediate values. Based on the available data, a linear function can be proposed for the estimation of c_β as a function of S, i.e., $c_\beta = 0.44 + 0.004S$ ($\gamma_{\beta sEBV} = (1 - c_\beta)\cos^2\beta + c_\beta$). This means that c_β varies linearly between 0.44 for $S = 0$ and 0.60 for $S = 40$. In other words, the more spreading, the smaller the effect of wave obliquity, which is physically sound as more spreading means that waves are coming from different directions. As seen, $\gamma_{\beta sEBV}$ considers the quantitative effect of wave angle and wave spreading.

The accuracy metrics of this reduction factor for different datasets are shown in the last column of Tables 5 and 6. As seen, the proposed formula provides reasonable results for considering wave spreading in oblique waves. For more investigation, the accuracy metrics (*NBias* and *SI*) of these reduction factors for different range of β and S are shown in the Figures 8 and 9. It can be concluded that the new reduction factor has more accurate prediction in almost all wave angles (except $\beta = 30$) and in all wave spreading situations (except $S = 10$) than others. The accuracy in the prediction is seen also in the Figure 10 and the scatter in the data is reduced in this way.
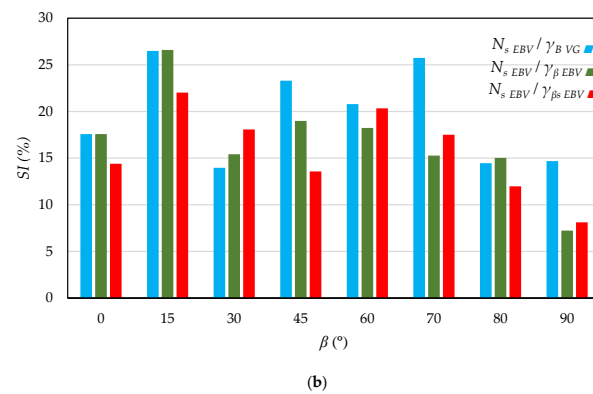

Figure 8. *Cont.*

(**b**)

Figure 8. Accuracy metrics of $N_{S\ EBV}$ using the new and Van Gent [19] wave obliquity reduction factors for different ranges of β in the expressions by EBV, (**a**) *NBias* and (**b**) *SI*.
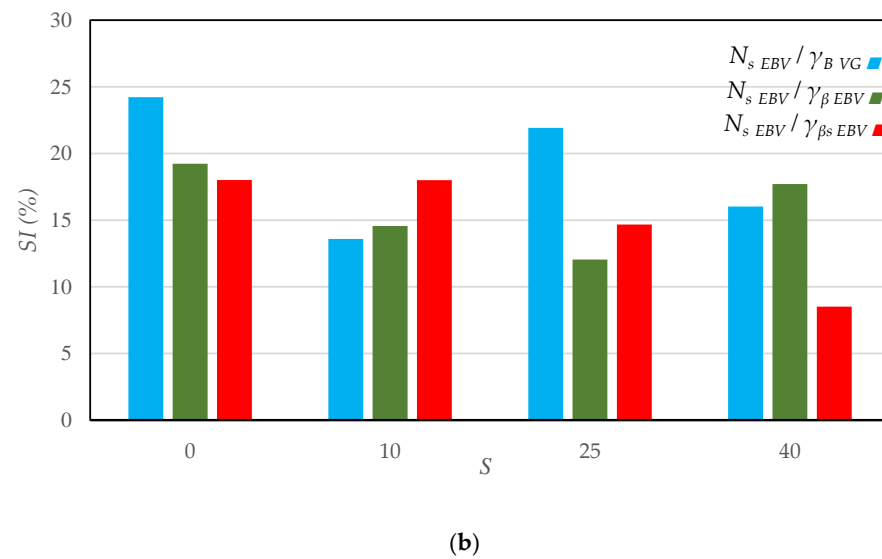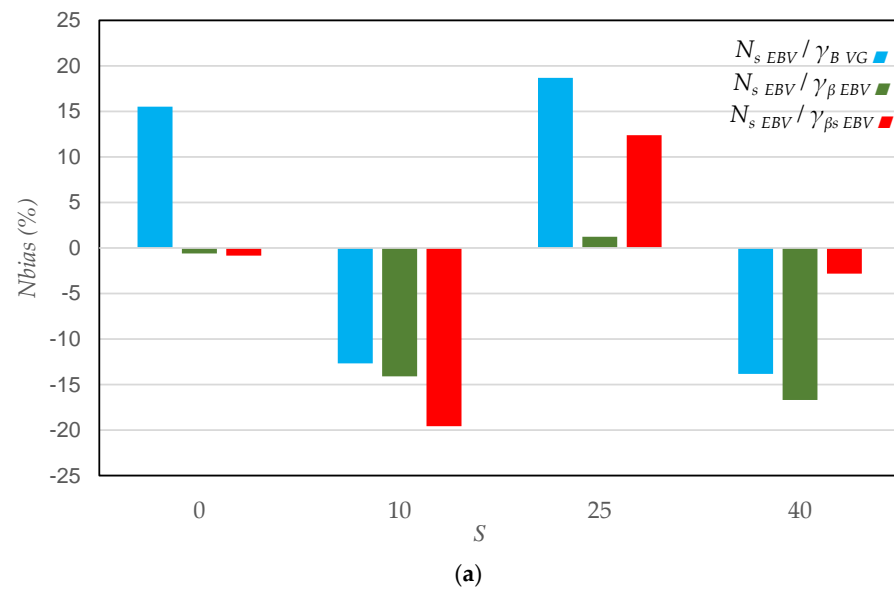

(**a**)

(**b**)

Figure 9. Accuracy metrics of $N_{S\ EBV}$ using the new and Van Gent [19] wave obliquity reduction factors for different ranges of *S* in the expressions by EBV, (**a**) *NBias* and (**b**) *SI*.
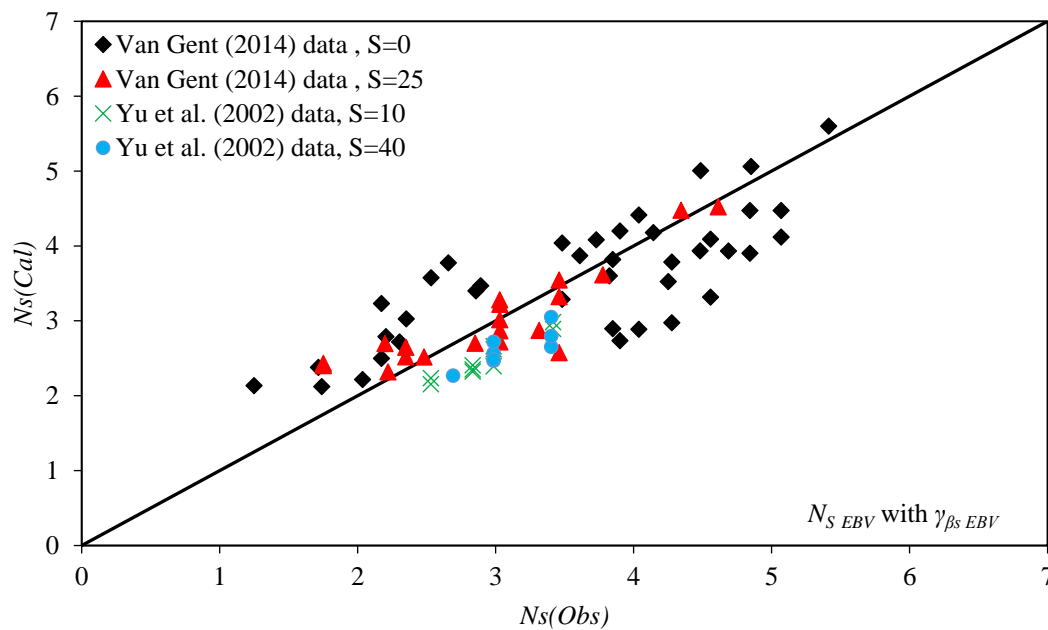
Figure 10. Comparison between measured and predicted (by EBV) stability numbers using the new reduction factor ($\gamma_{\beta s\ EBV}$). Black diamond and red triangle: Van Gent [19], green multiplication and blue circle: Yu et al. [17].

Figure 11 displays the effects of wave direction and spreading on the reduction in required armour size. As seen, an increase in wave spreading leads to a reduction in required armour size. For example, for a wave angle of 40° and wave spreading of 30, the reduction factor of the armour size is 0.8. Hence, the armour size calculated based on Etemad-Shahidi et al. [1] can be decreased by 20%.
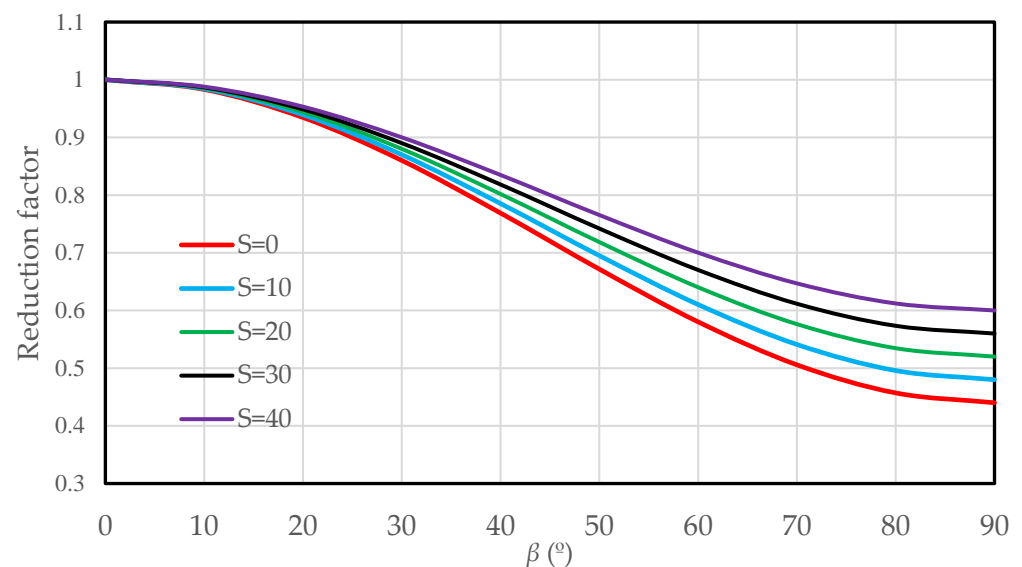

Figure 11. Reduction factor of armour size due to the wave obliquity and different spreading values.

4. Summary and Conclusions

One of the most recent formulae for estimating the stability of rock-armoured slopes is Etemad-Shahidi et al. [1], or EBV. The aim of this study was to develop a suitable wave obliquity reduction factor for the EBV stability formula. Hence, the influence of oblique waves on the stability of the rock armour layer has been investigated based on the available dataset. Data records of Yu et al. [17] and Van Gent [19], with damage levels in the range

of $2 \leq S_d \leq 12$, were selected. These studies show that the influence of oblique waves on the stability of rock armour layers is significant, and the required armour size can be reduced, compared to the perpendicular wave attack case. This effect can be considered the reduction factor γ_β for the required armour size which can reduce construction costs. For example, a 15% reduction in armour size will result in about a 40% reduction in the armour's weight, which is significant.

All available γ_β formulae were evaluated in combination with the EBV stability formula using different datasets separately, and it was concluded that the Van Gent [19] approach provides more accurate predictions than the others. Based on their approach, an appropriate and compatible reduction factor for the EBV stability formula was developed, which includes the effect of directional spreading explicitly for the first time. It was concluded that the results are improved slightly by using the new and more physically sound wave obliquity reduction factor.

In this study, one of the most recent formulae for estimating the stability of rock-armoured slopes was extended by considering the effects of the wave angle and the directional spreading coefficient. The results show that the prediction is more accurate and reliable when using an expression calibrated for the mentioned stability formula. The newly proposed reduction formula, $\gamma_{\beta sEBV} = (1 - c_\beta)\cos^2\beta + c_\beta$ with $c_\beta = 0.44 + 0.004S$, leads to an unbiased prediction and a 30% improvement in *SI*, with a coefficient of variation of 19%. It should be noted that the effect of wave multi-directionality on stability has been quantified explicitly for the first time.

Author Contributions: M.B.: Conceptualization, Writing—original draft Validation, Formal analysis. A.E.-S.: Conceptualization, Methodology, Writing—review & editing, M.R.A.v.G.: Data curation, Writing—review & editing, Conceptualization. All authors have read and agreed to the published version of the manuscript.

Institutional Review Board Statement: Not applicable.

Informed Consent Statement: Not applicable.

Data Availability Statement: Data are available upon reasonable request.

Conflicts of Interest: The authors declare no conflict of interest.

Nomenclature

Symbol	Name	Unit
α	Structure slope angle	[°]
β	Wave angle	[°]
C_P	Permeability coefficient	[-]
CC	Correlation coefficient	[-]
$\Delta = (\rho_s/\rho_w) - 1$	Relative buoyant mass density	[-]
$D_{n50} = (M_{50}/\rho_a)^{1/3}$	Armour equivalent cube length exceeded by 50% of a sample by weight	[m]
D_{50}	Equivalent spherical diameter	[m]
D_{n50c}	Core equivalent cube length exceeded by 50% of a sample by weight	[m]
EBV	Etemad-Shahidi et al. [1]	[-]
$\gamma_{\beta\ EBV}$	New wave angle and spreading reduction factor which is a function of β (quantitatively) and S (qualitatively) for EBV formula	[-]
$\gamma_{\beta S\ EBV}$	New wave angle and spreading reduction factor which is a function of β (quantitatively) and S (quantitatively) for EBV formula	[-]
γ_{BVG}	Wave angle and spreading reduction factor suggested by Van Gent [19]	[-]
H_{m0}	Significant wave height based on frequency domain analysis	[m]

$H_{2\%}$	Average of the highest 2% of incident waves	[m]
H_{50}	Average of the 50 highest waves	[m]
H_s	Significant wave height at toe of the structure	[m]
h	Water depth	
K_D	Hudson stability coefficient	[-]
$Ir_{m-1,0}$	Iribarrn number based on $T_{m-1,0}$.	[-]
I_{rc}	Transition Iribarrn number in VSK formula	[-]
m_i	Measured values	[-]
$\overline{m_i}$	Average of the measured values	[-]
M_{50}	Median rock mass	[kg]
n	The number of observations	[-]
N_w	Number of wave attack	[-]
N_s	Stability number using Hs	[-]
$N_{S\,EBV}$	Stability number calculated by EBV formula	[-]
$N_{S\,VSK}$	Stability number calculated by VSK formula	[-]
$N_{s\,Measured}$	Measured stability number	
N_{50}	Stability number using H_{50}	[-]
P	Nominal permeability	[-]
P_i	Predicted values	[-]
R_c	Crest freeboard	[m]
ρ_s	Rock density	[kg/m^3]
ρ_w	Water density	[kg/m^3]
$S_{om} = 2\pi H_{mo}/gT_{om}^2$	Deep water wave steepness using T_{om}	[-]
$S_{om-1,0}$	Deep water mean wave steepness using $T_{-1,0}$	[-]
S_d	Damage level	[-]
SI	Scatter index	[-]
$T_{m-1,0} = m_{-1}/m_0$	Mean energy wave period based on frequency domain	[s]
T_P	Peak wave period	[s]
T_m	Mean wave period	[s]
$T_{m-1,0,deep}$	Mean energy wave period based on frequency domain analysis in deep water	[s]
VSK	Van Gent et al. [22]	[-]
VG	Van Gent [19]	
WV	Wolters and Van Gent [18]	[-]

References

1. Etemad-Shahidi, A.; Bali, M.; van Gent, M.R.A. On the stability of rock armored rubble mound structures. *Coast. Eng.* **2020**, *158*, 103655.
2. Kolahdoozan, M.; Bali, M.; Rezaee, M.; Moeini, M.H. Wave-transmission prediction of π-type floating breakwaters in intermediate waters. *J. Coast. Res.* **2017**, *33*, 1460–1466. [CrossRef]
3. Han, M.; Wang, C. Hydrodynamics study on rectangular porous breakwater with horizontal internal water channels. *J. Ocean Eng. Mar. Energy* **2020**, *6*, 377–398. [CrossRef]
4. Wang, C.M.; Han, M.M.; Lyu, J.; Duan, W.H.; Jung, K.H.; Kang An, S. Floating forest: A novel concept of floating breakwater-windbreak structure. In *WCFS2019: Proceedings of the World Conference on Floating Solutions*; Springer: Singapore, 2020; pp. 219–234.
5. Rahman, S.; Baeda, A.; Achmad, A.; Jamal, R. Performance of a New Floating Breakwater. In *IOP Conference Series: Materials Science and Engineering*; IOP Publishing: Bristol, UK, 2020; p. 012081.
6. Zhu, Y.; Tang, H. Automatic Damage Detection and Diagnosis for Hydraulic Structures Using Drones and Artificial Intelligence Techniques. *Remote Sens.* **2023**, *15*, 615. [CrossRef]
7. Gao, J.; Ma, X.; Dong, G.; Chen, H.; Liu, Q.; Zang, J. Investigation on the effects of Bragg reflection on harbor oscillations. *Coast. Eng.* **2021**, *170*, 103977. [CrossRef]
8. Karimaei Tabarestani, M.; Feizi, A.; Bali, M. Reliability-based design and sensitivity analysis of rock armors for rubble-mound breakwater. *J. Braz. Soc. Mech. Sci. Eng.* **2020**, *42*, 136. [CrossRef]
9. Etemad-Shahidi, A.; Bali, M.; van Gent, M.R.A. On the toe stability of rubble mound structures. *Coast. Eng.* **2021**, *164*, 103835. [CrossRef]
10. Etemad-Shahidi, A.; Koosheh, A.; van Gent, M.R.A. On the mean overtopping rate of rubble mound structures. *Coast. Eng.* **2022**, *177*, 104150. [CrossRef]

11. Houtzager, D.; Hofland, B.; Caldera, G.; van der Lem, C.; van Gent, M.; Bakker, P.; Antonini, A. Embedded rocking measurement of single layer armour units: Development and first results. In Proceedings of the ICE Breakwaters 2023: Coasts, Marine Structures and Breakwaters, Portsmouth, UK, 25–27 April 2023.
12. De Waal, J.; Van der Meer, J. Wave runup and overtopping on coastal structures. In Proceedings of the 23rd International Conference on Coastal Engineering, Venice, Italy, 4–9 October 1992; pp. 1758–1771.
13. Galland, J.-C. Rubble mound breakwater stability under oblique waves: An experimental study. In Proceedings of the 24th International Conference on Coastal Engineering, Kobe, Japan, 23–28 October 1994; pp. 1061–1074.
14. Hebsgaard, M.; Sloth, P.; Juhl, J. Wave overtopping of rubble mound breakwaters. In Proceedings of the 26th International Conference on Coastal Engineering, Copenhagen, Denmark, 22–26 June 1998; pp. 2235–2248.
15. Andersen, T.L.; Burcharth, H.F. Three-dimensional investigations of wave overtopping on rubble mound structures. *Coast. Eng.* **2009**, *56*, 180–189. [CrossRef]
16. Nørgaard, J.Q.H.; Andersen, T.L.; Burcharth, H.F.; Steendam, G.J. Analysis of overtopping flow on sea dikes in oblique and short-crested waves. *Coast. Eng.* **2013**, *76*, 43–54. [CrossRef]
17. Yu, Y.-X.; Liu, S.-X.; Zhu, C.-H. Stability of armour units on rubble mound breakwater under multi-directional waves. *Coast. Eng. J.* **2002**, *44*, 179–201. [CrossRef]
18. Wolters, G.; Van Gent, M. Oblique wave attack on cube and rock armoured rubble mound breakwaters. *Coast. Eng. Proc.* **2011**, *32*, 34. [CrossRef]
19. Van Gent, M.R.A. Oblique wave attack on rubble mound breakwaters. *Coast. Eng.* **2014**, *88*, 43–54. [CrossRef]
20. Hudson, R. *Design of Quarry-Stone Cover Layers for Rubble-Mound Breakwaters*; Coastal Engineering Research Centre: Vicksburg, MS, USA, 1958.
21. Van der Meer, J.W. Deterministic and probabilistic design of breakwater armor layers. *J. Waterw. Port Coast. Ocean Eng.* **1988**, *114*, 66–80. [CrossRef]
22. Van Gent, M.R.A.; Smale, A.J.; Kuiper, C. Stability of rock slopes with shallow foreshores. In Proceedings of the Coastal Structures 2003, Portland, OR, USA, 26–30 August 2003; pp. 100–112.
23. Etemad-Shahidi, A.; Bali, M. Stability of rubble-mound breakwater using H50 wave height parameter. *Coast. Eng.* **2012**, *59*, 38–45. [CrossRef]
24. Van der Meer, J. Stability of rubble mound revetments and breakwaters. In *Developments in Breakwaters*; ICE Publishing: London, UK, 1985; pp. 191–202.
25. The Rock Manual. The Use of Rock in Hydraulic Engineering. CIRIA-CUR, Publication C683. 2007. Available online: https://www.kennisbank-waterbouw.nl/DesignCodes/rockmanual/introduction.pdf (accessed on 31 May 2023).
26. Sigurdarson, S.; van der Meer, J. Design and Construction Aspects of Berm Breakwaters. In *Coastal Structures and Solutions to Coastal Disasters 2015: Resilient Coastal Communities*; American Society of Civil Engineers: Reston, VA, USA, 2017; pp. 864–875.
27. U.S. Army Corps of Engineers. Coastal Engineering Manual (CEM), Engineer Manual 1110-2-1100, 2002, Washington, DC (6 volumes) 2011: US. Chapter VI, Part 5. Available online: https://www.publications.usace.army.mil/USACE-Publications/Engineer-Manuals/u43544q/636F617374616C20656E67696E656572696E67206D616E75616C/ (accessed on 30 April 2023).